

## Shell Structure and Electronic Excitations of Quantum Dots in a Magnetic Field Probed by Inelastic Light Scattering

D. J. Lockwood,<sup>1</sup> P. Hawrylak,<sup>1</sup> P. D. Wang,<sup>2</sup> C. M. Sotomayor Torres,<sup>3</sup> A. Pinczuk,<sup>4</sup> and B. S. Dennis<sup>4</sup>

<sup>1</sup>*Institute for Microstructural Sciences, National Research Council of Canada, Ottawa, Ontario, Canada K1A 0R6*

<sup>2</sup>*Department of Electrical Engineering, Notre Dame University, Notre Dame, Indiana 46556*

<sup>3</sup>*Naanoelectronics Research Center, Glasgow University, Glasgow, United Kingdom*

<sup>4</sup>*AT&T Bell Laboratories, Murray Hill, New Jersey 07974*

(Received 28 December 1995; revised manuscript received 15 April 1996)

Inelastic light scattering experiments on deep-etched GaAs/AlGaAs modulation doped quantum dots in a magnetic field are reported. The Raman measurements at large in-plane wave vector transfer reveal a multicomponent excitation spectrum of the many-electron quantum dots. Observed transitions split with the magnetic field. The experimental results are interpreted in terms of the calculated excitation spectrum in the Hartree approximation. The results reveal an electronic shell structure of quantum dots and a low energy excitation due to a Landau-like band crossing the Fermi level with increasing magnetic field. [S0031-9007(96)00625-4]

PACS numbers: 73.20.Dx, 71.45.Gm, 78.66.Fd, 78.30.Fs

Quantum dots (QD) are formed by laterally confining a quasi-two-dimensional electron gas [1]. The quantization of the kinetic energy leads to a discrete density of states characteristic of atoms and hence QD's can be thought of as artificial atoms with a well controlled number of electrons. Because QD's are embedded in a semiconductor matrix, their electronic excitations can be drastically modified by magnetic fields. The magnetic field and the electron-electron interactions lead to a range of interesting ground states. In a strong magnetic field these ground states are analogs of the chiral Luttinger liquid [2–6] and, in even stronger magnetic fields, of incompressible liquids of the fractional quantum Hall effect [7–9]. These different ground states possess a spectrum of characteristic charge and spin density excitations. At present, very little is known about these excitations as the experimental techniques employed so far [8,10–17] probe mainly ground state properties of quantum dots.

Inelastic light scattering measures the excitation spectrum of a QD [18–21] and, in principle, can provide direct evidence of the discrete nature of excitations in zero-dimensional (0D) systems and of the effects of electron-electron interactions. In the absence of a magnetic field, Strentz *et al.* [21] measured the resonant electronic Raman spectrum from shallow etched QD's with sizes down to 400 nm while Wang *et al.* [19] measured the resonant electronic Raman spectrum of deep etched modulation-doped QD's with sizes down to 100 nm. Both groups attributed structures in the Raman spectra to the 0D density of states.

In this Letter we present measurements and theoretical interpretations of inelastic light scattering spectra of electronic excitations in GaAs quantum dots in large magnetic fields. These spectra display a complex set of elementary excitations in correspondence with transitions between the energy levels within the quasi-0D electron system in a magnetic field. These results are evidence of novel appli-

cations of inelastic light scattering in studies of quantum confinement and electron interactions. Such applications emerge from the relatively large wave-vector transfer in these optical experiments that correspond to wavelengths comparable to radii of QD's. In this wave vector regime the generalized Kohn theorem [13,15], which limits the reach of long wavelength probes such as far infrared (FIR) spectroscopy, is no longer valid, and the light scattering method is found to be effective in giving access to excitations that display the combined effects of the confining potentials and electron-electron interactions [18]. The results presented below reveal a complex shell structure in the states of quantum dots with many electrons.

The GaAs/GaAlAs quantum dots were prepared in the form of disks of radius  $R$ . Disks with radii in the range  $50 < R < 100$  nm were etched from a modulation doped multi-quantum-well structure [19] with carrier density  $n_s = 8.5 \times 10^{11} \text{ cm}^{-2}$ . The photoluminescence and near-resonant electronic Raman spectra (in a backscattering geometry) of the deep-etched quantum dots were measured in magnetic fields up to 12 T at 2 K. A rich spectrum of excitations with Raman shifts in the range 1–35 meV was observed in each sample.

Spectra for a dot with a nominal radius  $R = 75$  nm and nominal density  $n_s = 8.5 \times 10^{11} \text{ cm}^{-2}$  in magnetic fields  $B = 0$ –12 T are shown in Fig. 1. The  $B = 0$  spectra show clearly broad peaks separated by approximately  $\omega_0 = 6$  meV as indicated by arrows. Up to three peaks were observed. On top of the broad structure a number of sharper peaks, especially at low energies, is also visible. A similar structure was observed previously [19,21] in other dot structures. We find that  $\omega_0(R)$  decreases with the increasing size of quantum dots ( $R = 50$  nm,  $\omega_0 = 8$  meV;  $R = 75$  nm,  $\omega_0 = 6$  meV;  $R = 100$  nm,  $\omega_0 = 4.5$  meV), but no simple dependence on size can be formulated yet.

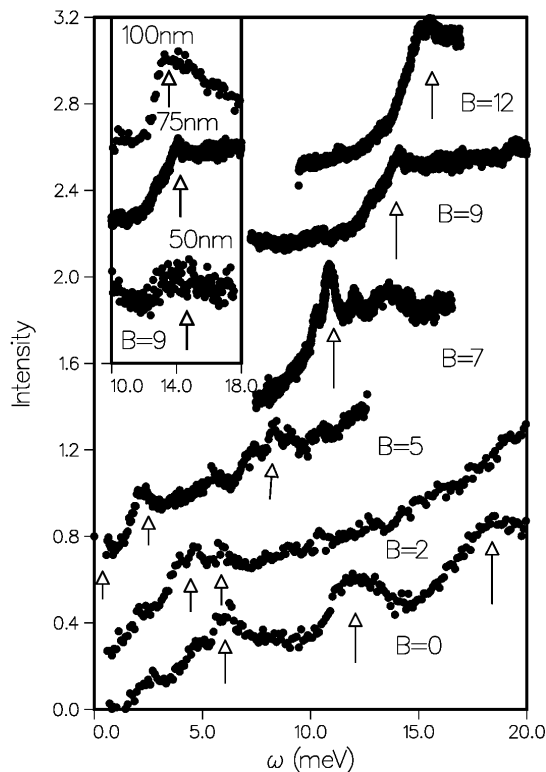


FIG. 1. Measured Raman spectra of quantum dots with nominal carrier density  $n_s = 8.5 \times 10^{11} \text{ cm}^{-2}$  and radius  $r = 75 \text{ nm}$  for magnetic fields  $B = 0-12 \text{ T}$ . The inset shows transitions  $\Omega_+$  at  $B = 9 \text{ T}$  for dot radii  $R = 50, 75, 100 \text{ nm}$ .

As the magnetic field increases, the spectrum evolves in a complicated way. For example, the lowest peak appears to split and evolves into two peaks  $\Omega_{+/-}$  as indicated by arrows. However, the  $\Omega_+$  peak at  $B = 5 \text{ T}$  is split into a number of peaks, and an additional low energy peak appears. This complicated behavior can only be understood by a comparison of experiment with realistic calculations of Raman spectra. Some features, e.g., the decrease (increase) of the  $\Omega_-$  ( $\Omega_+$ ) transitions with increasing magnetic field, can be understood by comparison with FIR spectroscopy [13], where the  $\Omega_-$  and  $\Omega_+$  peaks can be associated with the intra-Landau and inter-Landau level transitions of a quantum dot. The decrease of the high energy peak with increasing dot size for a fixed magnetic field  $B = 9 \text{ T}$  is shown in the inset for dot radii  $R = 50, 75,$  and  $100 \text{ nm}$ .

The exciting light is scattered by a 2D array of pillars, each containing ten QD's. Not surprisingly [22], the spectra do not show the wave-vector conservation and clear polarization dependence found in quantum well experiments. Thus the spin density (SDE) and charge density (CDE) excitations are not resolvable from the single particle excitations (SPE), which dominate the electronic Raman spectrum of the unpatterned quantum wells. In the interpretation of the experimental spectra, we initially

restrict ourselves to the analysis of the dominant SPE based on Hartree calculations. In the absence of the wave-vector conservation the cross section  $I(\omega)$  is averaged over all possible wave-vector transfers  $q = k_f - k_i$  of the incident ( $k_i$ ) and scattered ( $k_f$ ) light:  $I(\omega) \approx \sum_q W(q)I(q, \omega)$ . The function  $W(q)$  depends on the structure of individual dots and the structure of an array of pillars on the sample surface. The Raman cross section  $I(q, \omega)$  for a given wave-vector transfer  $q$  and frequency  $\omega$  is proportional to the imaginary part of the polarizability  $\Pi(q, \omega)$  of the system [23]:

$$I(q, \omega) \approx \sum_{m, m', \nu, \nu'} |\langle m', \nu' | \rho_q | m, \nu \rangle|^2 [1 - f(m', \nu')] \times f(m, \nu) \delta(E_{m'}^{\nu'} - E_m^\nu - \omega), \quad (1)$$

where the density operator  $\rho_q = e^{i\vec{q}\cdot\vec{r}}$ , and  $f(m, \nu)$  is the Fermi occupation function for a state  $\nu$  with angular momentum  $m$  and energy  $E_m^\nu$ . The coupling through the density fluctuation operator  $e^{i\vec{q}\cdot\vec{r}} = \sum_m i^m e^{im\theta} J_m(qr)$  induces transitions between different angular momenta  $m$  and different single particle states  $\nu$ . To calculate the wave functions, energies, and SPE spectra we approximate the quantum dots as disks of radius  $R$  and thickness  $t$ , confined by infinite potential barriers. The positive charges of ionized donors are modeled as a disk with uniform density, separated by a distance  $d$  from the plane of the dot. For such a high density multiple-quantum-well system, we assume that electrons trapped in surface states represent a very small fraction of the free electrons.

In the Hartree approximation, the many-electron Hamiltonian for free electrons is replaced by a Hamiltonian of a single particle moving in a confining potential and a self-consistent Hartree potential determined by the electron and the positive charge density through electron-electron and electron-positive charge Coulomb interactions. The electron density is given in terms of occupied eigenstates  $\Psi_\nu^m$  of the Hartree Hamiltonian.

In numerical results the following parameters were used:  $R = 70 \text{ nm}$ ,  $N_e = 124$ ,  $d = 30 \text{ nm}$ ,  $t = 8 \text{ nm}$ . These parameters correspond to a disk with a diameter of  $140 \text{ nm}$  and density  $n_s \approx 8 \times 10^{11} \text{ cm}^{-2}$ . In calculating Coulomb interactions we have also assumed a uniform dielectric constant of GaAs and neglected the effects due to image charges associated with the semiconductor-vacuum interface.

The results of the calculations are illustrated in Fig. 2 which shows the energy levels  $E(m, \nu)$  and the corresponding (Gaussian broadened) density of states  $D(\omega)$  of the dot for magnetic fields  $B = 0, 5 \text{ T}$ . The energy spectrum for  $B = 0 \text{ T}$  is discrete and hence the 0D density of states (DOS) consists of a series of peaks. There is a typical single particle energy spacing  $\delta E \approx 0.1-0.5 \text{ meV}$  within each peak and an overall arrangement of peaks in the DOS reminiscent of the shell structure of atoms, with a typical energy spacing of  $\approx 5 \text{ meV}$ .

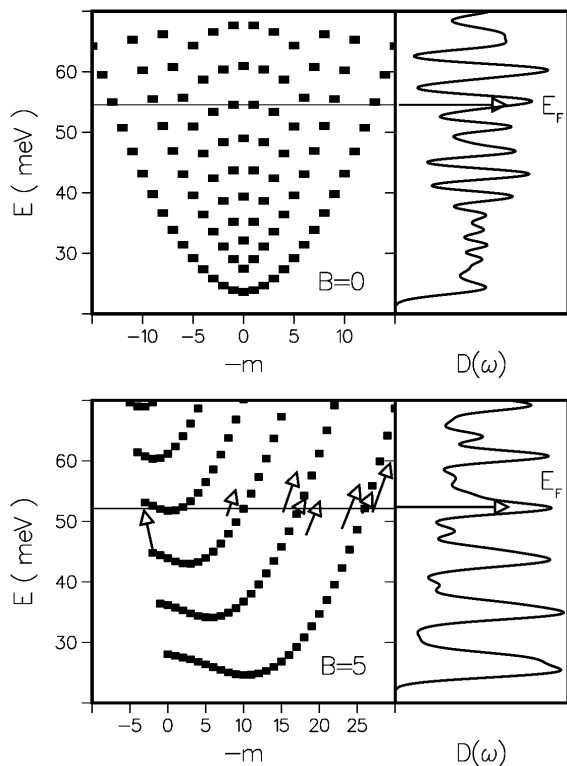


FIG. 2. Hartree energy levels  $E_m^v$  and density of states  $D(\omega)$  of a dot for magnetic fields  $B = 0$  and 5 T. The horizontal line indicates the Fermi level and arrows indicate strong Raman transitions for  $qR = 3.5$  across the Fermi level at  $B = 5$  T.

When compared with the DOS of noninteracting electrons we find that the modulation is enhanced by electron-electron interactions. This is due to the spatial separation of the positive background from the disk. Since electrons repel each other very effectively, the electron charge density is depressed inside the disk and enhanced at the edges of the disk. The Hartree potential is therefore repulsive in the center of the dot, a situation very similar to Hartree potentials in modulation-doped quantum wells. This is in stark contrast to the normally assumed parabolic confining potential. The shell structure is enhanced by the degeneracy of states with the same absolute value of angular momentum  $m$ . This degeneracy is removed by the magnetic field, leading to a splitting of energy levels. For small values of the magnetic field a rapid rearrangement and crossing of levels takes place. For higher magnetic fields,  $B > 4$  T, Landau bands begin to form as shown in Fig. 2 for  $B = 5$  T.

One finds a single particle energy spacing within each Landau band from  $\delta E \approx 0.1$  meV close to the center of the dot (small  $|m|$ ) to a spacing  $\delta E \approx 5$  meV for large angular momenta, i.e., edge states. The Landau bands have a negative dispersion for small  $m$  as they follow the effective Hartree potential, which is repulsive for electrons in the center of the dot, and a positive dispersion when electrons approach a potential barrier at the edge. The turning point marks the peak in DOS. As

a result, the Fermi level crossing the Landau band gives rise to very low frequency excitations ( $|m| \approx 2$  in Fig. 2). The remaining excitations are either edge intra-Landau band excitations and inter-Landau level excitations. In Fig. 2 we show SPE with significant oscillator strength for magnetic field  $B = 5$  T and a selected wave-vector transfer  $qR = 3.5$ . The Fermi level is indicated with a solid line, and transitions between initial and final states are indicated with arrows. We see, surprisingly, that higher harmonics of edge excitations fall into the same energy range and have the same oscillator strength as inter-Landau band excitations.

We now summarize in Fig. 3 the evolution with magnetic field of calculated SPE and measured Raman spectra. In the right panel of Fig. 3 we show representative calculated SPE spectra for small ( $qR = 0.7$ ;  $q = 1 \times 10^5$  cm $^{-1}$ ) and large ( $qR = 3.5$ ;  $q = 5 \times 10^5$  cm $^{-1}$ ) wave vectors involved in the scattering process. For comparison with experiment the calculated energies have been multiplied by a factor of 1.3 to account for a decrease in the effective dielectric constant due to the vacuum. The calculated spectra for  $q = 1 \times 10^5$  cm $^{-1}$  and  $B = 0$  show only one peak while

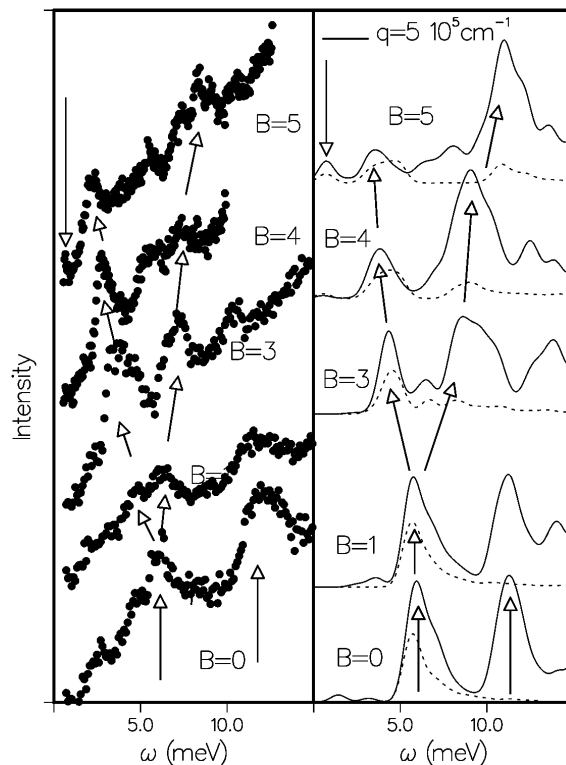


FIG. 3. (a) Measured Raman spectra of quantum dots with nominal carrier density  $n_s = 8.5 \times 10^{11}$  cm $^{-2}$  and radius  $r = 75$  nm for magnetic fields  $B = 0-5$  T. (b) Calculated SPE spectra  $I(q, \omega)$  of a dot with carrier density  $n_s = 8.0 \times 10^{11}$  cm $^{-2}$  ( $N = 124$ ) and radius  $r = 70$  nm, and  $q = 1 \times 10^5$  cm $^{-1}$  (dashed line) and  $q = 5 \times 10^5$  cm $^{-1}$  (solid line). The arrows point out related peaks in experiment and theory for each magnetic field.

spectra for  $q = 5 \times 10^5 \text{ cm}^{-1}$  consist of three main transitions with a spacing of the order of 6 meV in good agreement with experiment. If we follow the evolution of the calculated SPE spectrum as a function of the magnetic field, we see that the  $q = 5 \times 10^5 \text{ cm}^{-1}$  spectra are in agreement with the measured spectra. For example, at  $B = 1 \text{ T}$  we see two peaks, while at  $B = 3 \text{ T}$  we see three peaks. At  $B = 5 \text{ T}$  the agreement is also encouraging, especially with respect to the emergence of a very low energy excitation associated with the Fermi level crossing a quasi-Landau-level band. The measured spectra are, of course, an average over many such calculated spectra.

In summary, a very rich spectrum of excitations is revealed in the Raman spectrum of many-electron quantum dots in a magnetic field. The experimental spectra show a magnetic field behavior consistent with that calculated for single particle excitations within the Hartree approximation. The single particle excitation spectrum reflects the formation of electronic shells within quantum dots and exhibits a complex evolution with magnetic field. A realistic calculation of edge magnetoplasmons and spin density excitations, and of the mechanism of resonant excitation, is now required for a more detailed quantitative comparison with experiment, but the value of the inelastic light scattering technique in probing quantum dot excitations has been amply demonstrated. This now opens up the possibility to study collective excitations from a range of strongly correlated ground states in QD's in a strong magnetic field.

---

[1] For recent reviews and references, see M. Kastner, *Phys. Today* **46**, 24 (1993); T. Chakraborty, *Comments Condens. Matter Phys.* **16**, 35 (1992).

- [2] A. H. MacDonald *et al.*, *Aust. J. Phys.* **46**, 345 (1993).
- [3] C. de Chamon *et al.*, *Phys. Rev. B* **49**, 8227 (1994); J. J. Palacios *et al.*, *Europhys. Lett.* **23**, 495 (1993); C. de Chamon *et al.*, *Phys. Rev. B* **51**, 2363 (1995).
- [4] C. L. Kane *et al.*, *Phys. Rev. Lett.* **72**, 4129 (1994).
- [5] P. Hawrylak, *Phys. Rev. B* **51**, 17708 (1995).
- [6] J. H. Oaknin *et al.*, *Phys. Rev. Lett.* **74**, 5120 (1995).
- [7] P. A. Maksym, *Physica (Amsterdam)* **184B**, 385 (1993); P. A. Maksym *et al.*, *Phys. Rev. Lett.* **65**, 108 (1990).
- [8] P. Hawrylak, *Phys. Rev. Lett.* **71**, 3347 (1993).
- [9] J. J. Palacios *et al.*, *Phys. Rev. B* **50**, 5760 (1994).
- [10] O. Klein *et al.*, *Phys. Rev. Lett.* **74**, 785 (1995).
- [11] P. L. McEuen *et al.*, *Phys. Rev. B* **45**, 11419 (1992); A. S. Sachrajda *et al.*, *Phys. Rev. B* **47**, 6811 (1993).
- [12] J. Weis *et al.*, *Phys. Rev. Lett.* **71**, 4019 (1993).
- [13] B. Meuer *et al.*, *Phys. Rev. Lett.* **68**, 1371 (1992); Ch. Sikorski *et al.*, *Phys. Rev. Lett.* **62**, 2164 (1989); A. Lorke *et al.*, *Phys. Rev. Lett.* **64**, 2559 (1990).
- [14] R. C. Ashoori *et al.*, *Phys. Rev. Lett.* **71**, 613 (1993); Bo Su *et al.*, *Science* **255**, 313 (1992).
- [15] H. Drexel *et al.*, *Phys. Rev. Lett.* **73**, 2252 (1994).
- [16] P. Hawrylak *et al.*, *Phys. Rev. Lett.* **70**, 485 (1993).
- [17] S. Patel *et al.* (to be published).
- [18] P. Hawrylak, *Solid State Commun.* **93**, 915 (1995).
- [19] P. D. Wang *et al.*, *Superlattices Microstruct.* **15**, 23 (1994).
- [20] P. Hawrylak *et al.*, *Proceedings of the 11th International Conference on Electronic Properties of Two-Dimensional Systems*, Nottingham, 1995 (to be published).
- [21] R. Strenz *et al.*, *Phys. Rev. Lett.* **73**, 3022 (1994).
- [22] C. Dahl *et al.*, *Phys. Rev.* **51**, 17211 (1995).
- [23] A. Pinczuk and G. Abstreiter, in *Light Scattering in Solids*, edited by M. Cardona and G. Guntherodt (Springer, Berlin, 1989), p. 153; P. Hawrylak *et al.*, *Phys. Rev. B* **32**, 5169 (1985).